

Superconductivity of nano-TiO₂-added MgB₂

H. Kishan^a, V.P.S. Awana^{a,*}, T.M. de Oliveira^b, Sher Alam^c, M. Saito^c, O.F. de Lima^b

^a Superconductivity and Cryogenics Division, National Physical Laboratory, Dr. K.S. Krishnan Marg, New Delhi-110012, India

^b Instituto de Física “Gleb Wataghin”, UNICAMP, 13083-970, Campinas-SP, Brazil

^c CSSAG, National Institute of Materials Science (NIMS), 1-1, Namiki, Tsukuba 305-0046, Japan

Received 28 November 2006; received in revised form 26 February 2007; accepted 26 February 2007

Available online 2 March 2007

Abstract

We report on the synthesis, phase formation, microstructure, and magnetization, of nano(*n*)-TiO₂-added MgB₂ polycrystalline compounds. The added *n*-TiO₂ amounts are varied from 1% to 15% in weight (wt). All the studied samples are near single phase with small amounts of un-reacted Mg/MgO up to 10 wt%. The 15 wt% *n*-TiO₂ added sample seems to be a multi-phase compound with unusual broadening of the main MgB₂ reflection and additional unidentified lines in its X-ray diffraction (XRD) pattern. The superconducting transition temperature (*T*_c), as measured by magnetization experiments, decreases marginally with *n*-TiO₂ addition, for example the *T*_c are at 37.5 K and 35.5 K, respectively, for pristine and 10 wt% *n*-TiO₂-added samples. This indicates that Ti has not significantly substituted into the host MgB₂ lattice. The grain morphology of these compounds reveals porous regions and does not change much with TiO₂ addition. High resolution transmission electron microscopy (HRTEM) studies revealed the presence of *n*-TiO₂ in these samples. The critical current density (*J*_c) of the MgB₂-*n*-TiO₂ samples, as estimated using the Bean model, shows better performance under magnetic fields above 3 T than pristine MgB₂ for up to 4 wt% of addition, and decreases rapidly for additions above 6 wt%. We conclude that *n*-TiO₂ helps in enhancing the flux pinning centers in MgB₂ superconductor and hence improves the *J*_c(*H*) performance for additions up to 4 wt% in fields above 3 T.

© 2007 Elsevier B.V. All rights reserved.

Keywords: MgB₂; Nano-TiO₂ addition; Grains morphology and magnetization

1. Introduction

Since the discovery [1] of superconductivity at *T*_c ≈ 39 K in MgB₂, much attention has been paid to increasing the critical current density (*J*_c) of this compound via nano-particle additions. Basically, a relatively higher critical temperature (*T*_c) in comparison to non-HTSc (high temperature superconductor) and larger coherence length (ξ) than that of HTSc compounds make MgB₂ a suitable choice for practical applications. The relatively larger coherence length of up to 10–20 nm permits most commercially available nano-particles to act as pinning centers that lead to better performance in magnetic field for MgB₂. Accord-

ingly, several reports exist on nano-particle doped/added MgB₂ compounds [2–5].

In this article, we study the superconductivity of nano(*n*)-TiO₂-added MgB₂ superconductor. The *n*-TiO₂ powder used in the present study has an average grain size of 20 nm and was procured from Sigma–Aldrich. Our results indicated that the *J*_c values of *n*-TiO₂-added MgB₂ polycrystalline compounds, as estimated using the Bean model, shows better performance under magnetic field above 3 T than pristine MgB₂ for up to 4 wt% doping level, and thereafter decreases rapidly with further increase in TiO₂ amount.

2. Experimental

Our MgB₂ samples with additions of *n*-TiO₂ from 1 to 15 wt% were synthesized by encapsulation of well mixed

* Corresponding author. Fax: +91 11 25726938.

E-mail addresses: hkishan@mail.nplindia.ernet.in (H. Kishan), awana@mail.nplindia.ernet.in (V.P.S. Awana).

and palletized high quality (>3 N purity) Mg, B, and n -TiO₂ powders in a soft iron tube. Subsequently, the encapsulated samples were heated to 750 °C for two and half hours in an evacuated (10^{-5} Torr) quartz tube and, finally, they were quenched in liquid-nitrogen [6]. The X-ray diffraction patterns of the samples were recorded with a diffractometer using CuK_α radiation. SEM studies were carried out on these samples using a Leo 440 (Oxford Microscopy, UK) instrument. Electron diffraction (ED) and high resolution electron microscopy (HRTEM) were performed with an ultra-high voltage electron microscope (HVEM), a Hitachi H-1500, operated at 800 kV. The samples were crushed with a mortar into fine fragments in order to obtain fine edges and then ultrasonically dispersed in CCl₄ and transferred to carbon micro-grids. Simulations of ED patterns and HRTEM images based on dynamical diffraction theory were carried out using the software JEMS and Digital Micrograph. The Magnetization measurements were carried out with a *Quantum-Design PPMS-9T*.

3. Results and discussion

Fig. 1 depicts the room temperature X-ray diffraction (XRD) patterns of our MgB₂- n -TiO₂ samples with added ratios of n -TiO₂ from 0 to 15 wt%. The pristine compound crystallizes in hexagonal Bravais lattice with lattice parameters of $a = 3.0857(8)$ Å, and $c = 3.5230(8)$ Å. The compound is nearly single phase, except with some small impurity lines at around $2\theta \cong 36^\circ$ and 63° . The one at $2\theta \cong 36^\circ$ is due to a Mg metal [7] and the other at 63° is due to the presence of MgO, as suggested earlier by various authors [7,8]. Both the Mg and MgO peaks are marked in the pattern in Fig. 1. The c/a value of the pure compound is close to 1.14, which is known to be optimum for stoichiometric MgB₂ [9]. The main MgB₂ phase is preserved up to 10 wt% addition of n -TiO₂ with only a slight increase in the MgO concentration. The a and c lattice parameters calculated from identified MgB₂ peak positions decrease slightly up to 10 wt% addition. For example, they are $a = 3.0839(5)$ Å, and $c = 3.5167(9)$ Å for the 10 wt% MgB₂- n -TiO₂ sample. The small decrease in lattice parameters could occur due to formation of Mg_{1-x}B₂ [9]. This gets credence from the fact that with n -TiO₂ addition the formation of MgO increases and thus gives way to Mg_{1-x}B₂ formation. For the highest concentration of n -TiO₂ (see the upper most panel of Fig. 1) the main [101] reflection of MgB₂, at $2\theta = 42.52^\circ$, is clearly broadened due to the overlap with the main [200] reflection of MgO at $2\theta = 42.86^\circ$. Though a compositional analysis of these samples was not performed, the observed increase in MgO with n -TiO₂ addition might be due to the higher availability of oxygen released from TiO₂ in the encapsulated sample.

Scanning electron microscope (SEM) images at the same magnification are shown in Fig. 2a–c, respectively, for pristine, 4 wt%, and 15 wt% n -TiO₂-added samples. A homo-

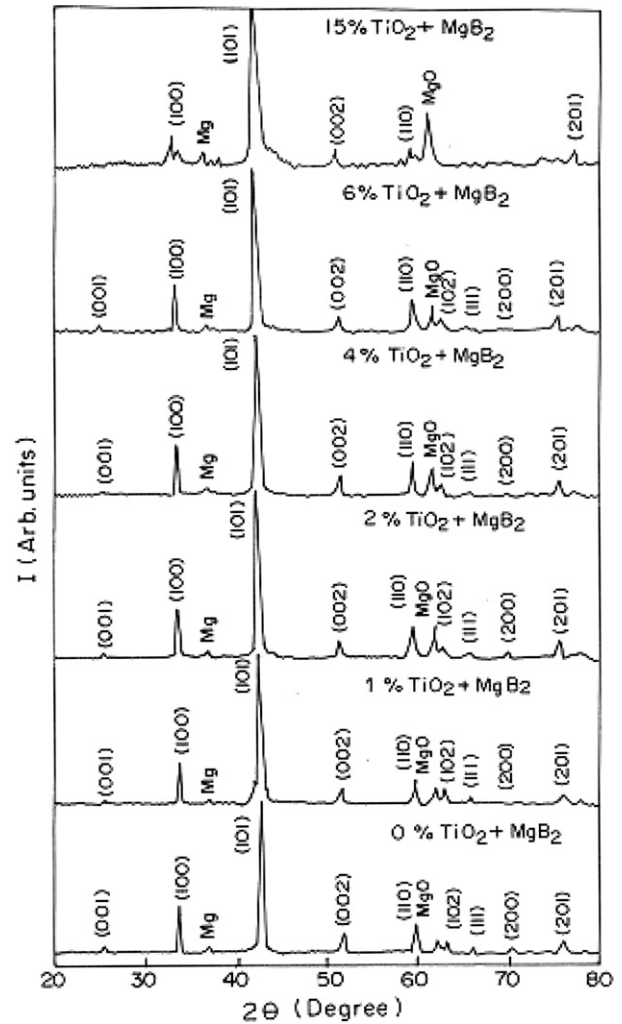


Fig. 1. Room temperature XRD patterns for various MgB₂- n -TiO₂ samples.

genous distribution of crystallites can be seen in the SEM pictures. The typical grain shape appears as platelets with sizes in the range of 1–3 μm. The shape and size of observed grains for our samples are in general agreement with results reported in the literature for MgB₂ [10]. Besides the MgB₂ grains, there are various porous regions visible in the micrographs of all samples irrespective of whether they are doped with n -TiO₂ or not. However, the distribution of n -TiO₂ is not seen at SEM resolution. To visualize the added n -TiO₂ particles with sizes up to 10–20 nm, we employed high resolution transmission electron microscopy (HRTEM).

The typical dark field image of the 6 wt% n -TiO₂-added sample is shown in Fig. 3a. Several black holes that appear in the image are presumably the n -TiO₂. The size of the n -TiO₂ particles is about to 10–15 nm. The ED pattern taken from these particles, shown in Fig. 3b and c, resembles that of the Rutile phase but is mixed with MgB₂ reflections. Both [100] axis (Fig. 3b) and ring-patterns (Fig. 3c) were inconclusive in separating the n -TiO₂ reflections. However, what could be confirmed from HRTEM studies

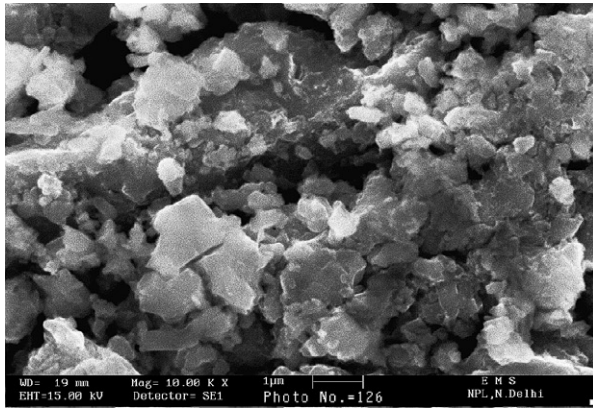
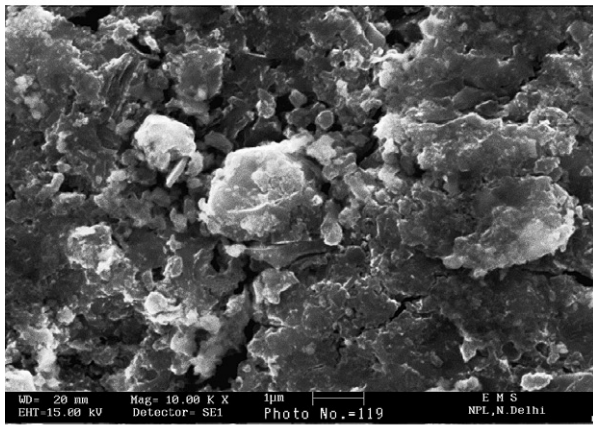
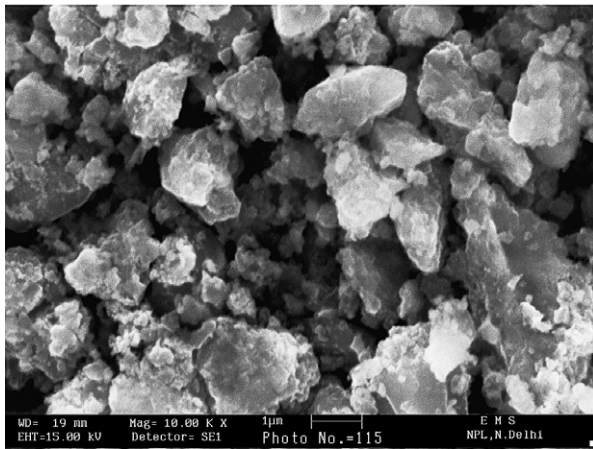
MgB₂ –PUREMgB₂ + 4% TiO₂MgB₂ + 15% TiO₂

Fig. 2. Scanning electron micrographs of various MgB₂–*n*-TiO₂ samples at the same magnification.

is that *n*-TiO₂ particles in the 10–15 nm size range are present in the sample.

DC magnetic susceptibility (χ) versus temperature (T) plots for the MgB₂–*n*-TiO₂ samples under an applied field of 10 Oe, in a zero-field-cooled (ZFC) state, are shown in Fig. 4. The field cooled (FC) data are not shown, because they are of very low magnitude and close to zero-base line.

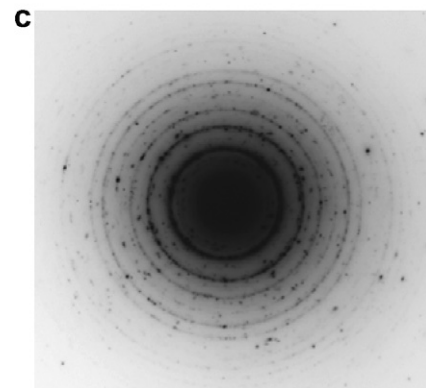
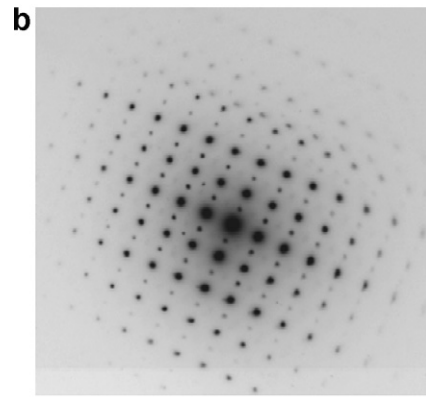
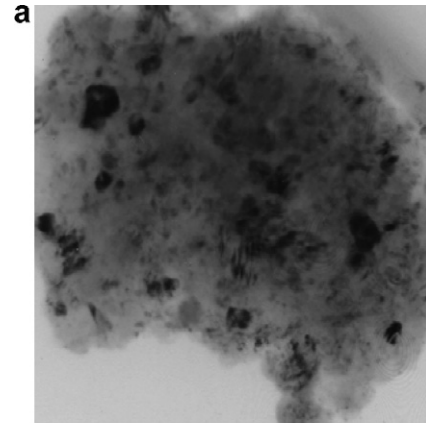


Fig. 3. (a) Dark field image showing *n*-TiO₂ holes, (b) [100] zone axis ED from dispersive *n*-TiO₂, and (c) ring patterns for *n*-TiO₂ from the 6 wt% *n*-TiO₂-added MgB₂ sample.

Further, the FC diamagnetic transitions are slightly broader and occur essentially at the same temperature as for ZFC, although the magnitude of the signal is very weak due to intense flux trapping. This indicates the presence of strong pinning centers inside the samples, which should favor high J_c values. It is evident from this figure that the pristine MgB₂ undergoes a sharp superconducting transition in ZFC mode at $T_c \approx 37.5$ K within less than a 1 K temperature interval. Then, without any usual rounding, the signal reaches an almost constant diamagnetic response all the way to lower temperatures. In fact, the diamagnetic signal remains more or less constant from 35 K down to 5 K for all *n*-TiO₂ additions up to 6 wt%. With the addition of *n*-TiO₂ up to 6 wt%, the critical temperature ($T_c \approx 37$ K)

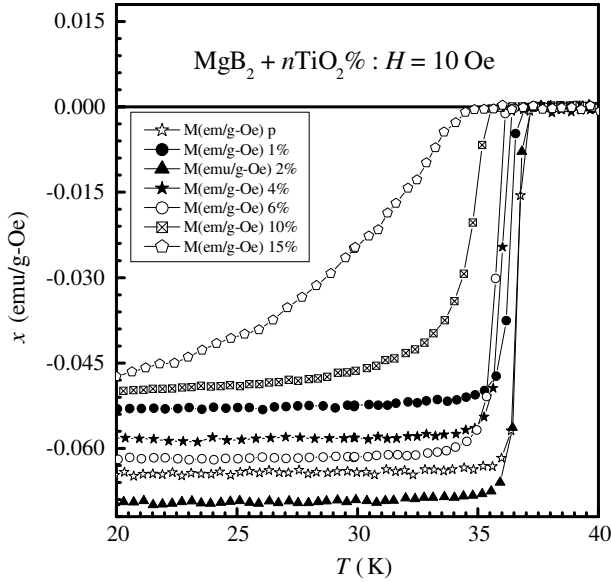


Fig. 4. Dc magnetic susceptibility, $\chi(T)$, behavior of various MgB_2 - n - TiO_2 samples.

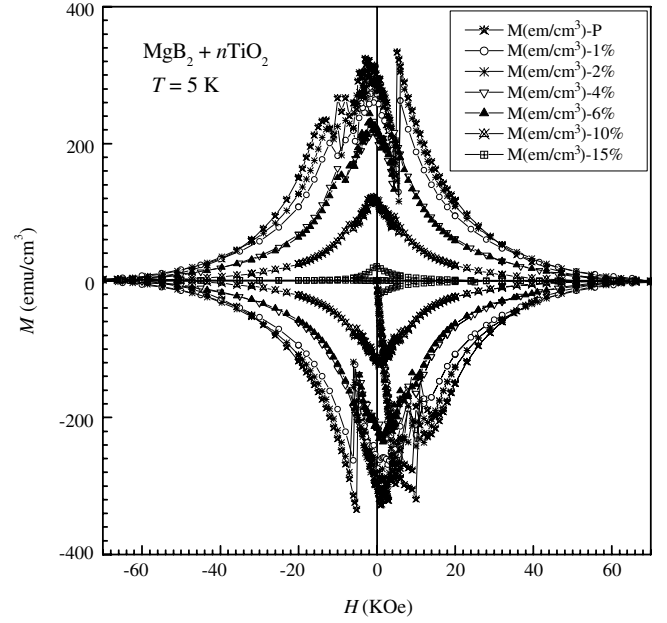


Fig. 5. Magnetization $M(H)$ plots of various MgB_2 - n - TiO_2 samples at $T = 5$ K.

remains within 1 K. However, it drops to 35.5 K for 10 wt% addition and to 33 K for 15 wt% addition, while the transitions become increasingly broader for these samples. These results indicate that n - TiO_2 remains almost as an inert additive in the host of MgB_2 at least up to 6 wt% doping. For higher additions of n - TiO_2 , there is a possibility of degrading the MgB_2 phase, thus producing lower T_c 's and broader transitions.

High field magnetization, $M(H)$, plots of our MgB_2 - n - TiO_2 samples are shown in Fig. 5 at 5 K under applied fields from -5 T to $+5$ T. In general the $M(H)$ loops are quite widely open, reaching maximum values around 300 emu/cm^3 for $|H| < 1$ T. An important feature seen in these data is the presence of fluxoid jumps in all samples below applied fields of about 2 T. Fluxoid jumps are also seen in high field magnetization $M(H)$ plots of our MgB_2 - n - TiO_2 samples at 10 K, but not at 20 K (plots not shown). Fluxoid jumps are often seen in high J_c MgB_2 samples in applied fields below 1–2 T [11–13]. Very recently, we observed that the flux avalanches seen in high J_c carrying MgB_2 are quite symmetric in both increasing/decreasing field in all four quadrants of the $M(H)$ loop [14]. The dynamics of sinusoidal-like symmetric reproducible flux avalanches was recently discussed by some of us [14].

Critical current densities (J_c) of the pristine and n - TiO_2 doped samples were estimated inductively from the $M(H)$ plots shown in Fig. 6a–c, by using the Bean critical state model [15]. For a cylindrical sample of diameter d this model predicts:

$$J_c = (30 \times \Delta M/d) \times (10/4\pi) (\text{A/cm}^2) \quad (1)$$

here, ΔM is the width of the $M(H)$ loop in emu/cm^3 units at a given field and temperature. Since the critical state of the flux density gradient occurs individually in each one of the

nearly uncoupled grains of the sample, it is reasonable to use the average grain size as a suitable value for d in Eq. (1), as has been done in other studies [2–5,13,14]. The calculated J_c values are plotted against field (H) in Fig. 6a–c for various MgB_2 - n - TiO_2 samples. It is seen that though the self-field J_c value is higher for the pristine undoped sample at 5 K, 10 K and 20 K, the $J_c(H)$ values are higher for the 1 wt%, 2 wt% and 4 wt% n - TiO_2 -added samples for $H > 3$ T, but decrease rapidly for additions above 6 wt%. For example, the $J_c(H)$ behavior of the 10 wt% and 15 wt% n - TiO_2 -added samples is quite inferior to that of pure and other doped samples. It seems that for higher n - TiO_2 added concentrations of more than 6 wt%, segregation on n - TiO_2 particles takes place and, hence, the pinning of vortices decreases. Also, the observed degradation of the MgB_2 phase for higher n - TiO_2 additions causes a reduction of T_c , thus acting as another mechanism for J_c weakening [16].

In conclusion, our results indicate that the MgB_2 - n - TiO_2 samples with 1–4 wt% of added TiO_2 nano-particles show effective pinning centers that improve substantially their $J_c(H)$ behavior. Also, the lattice, grain morphology and superconducting transition (T_c) are not significantly affected for n - TiO_2 particle additions up to about 6 wt%. Therefore, we conclude that an addition of up to 4 wt% TiO_2 nano-particles to a polycrystalline matrix of MgB_2 makes it potentially more attractive for technological applications. Furthermore, our results of nano(n)- TiO_2 -added MgB_2 superconductor are similar to those observed in another report by Xu et al. [11] on the same system. Though a host of different nano-particles have been doped into MgB_2 [2–5,11,12], the best performance yet seen is due to carbon derivatives [4,5]. The added n -carbon derivatives

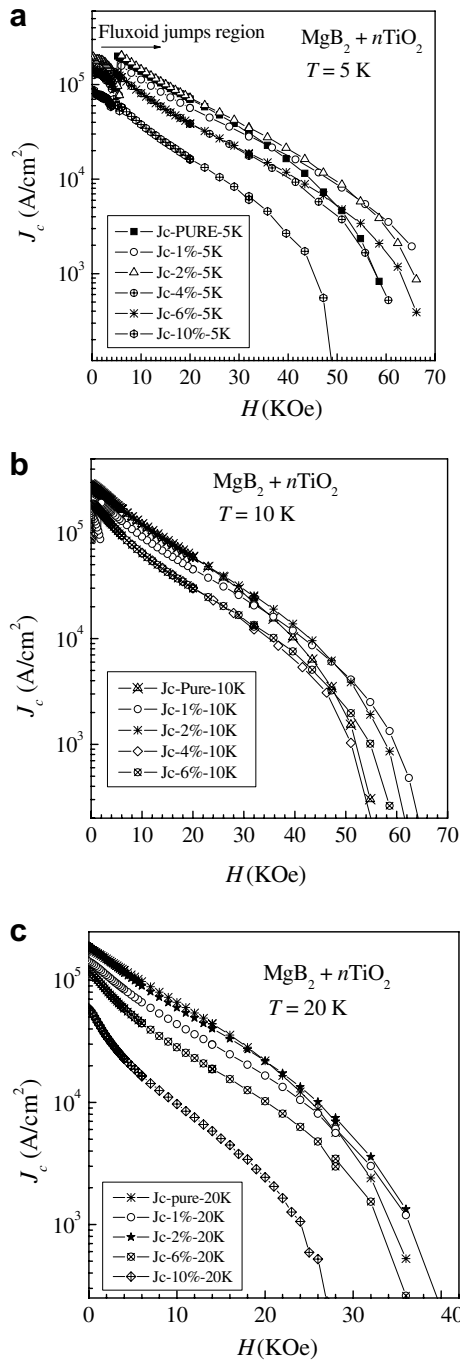


Fig. 6. Critical current density $J_c(H)$ plots for various MgB_2 - n - TiO_2 samples at (a) 5 K, (b) 10 K, and (c) 20 K.

[4,5] substituted to some extent on the B site in MgB_2 , while the rest remained as additive nano-particles within the MgB_2 grains. The former effect creates disorder in σ band superconducting condensate and the later provides effective pinning centers, thus both collectively improve the perfor-

mance of the doped system and, hence, are superior to other additives, such as reported in [11,12] and the present study.

Acknowledgement

This research is supported by the Indian National Science Academy (INSA)/Brazilian Science Agency (SBS) under the bilateral exchange program of scientists, through a visit of one of us (HK) to Unicamp, Brazil. The materials were synthesized in NPL India, and the magnetic characterization was done in Brazil. Authors from the NPL further appreciate the interest and advice given by our director Professor Vikram Kumar. The help from the NPL, SEM group is acknowledged for providing us with SEM analysis of our samples. OFL and TMO acknowledge financial support from the Brazilian Agencies, Fundação de Amparo a Pesquisa do Estado de São Paulo (FAPESP) and Conselho Nacional de Desenvolvimento Científico e Tecnológico (CNPq).

References

- [1] J. Nagamatsu, N. Nakagawa, T. Muranaka, Y. Zenitani, J. Akimitsu, Nature (London) 410 (2001) 63.
- [2] S.X. Dou, S. Soltanian, X.L. Wang, P. Munroe, S.H. Zhou, M. Ionescu, H.K. Liu, M. Tomsic, Appl. Phys. Lett. 81 (2002) 3419.
- [3] A. Matsumoto, H. Kumakura, H. Kitaguchi, H. Hatakeyama, Supercond. Sci. Technol. 16 (2003) 926.
- [4] S.X. Dou, W.K. Yeoh, J. Horvat, M. Ionescu, Appl. Phys. Lett. 83 (2003) 4993.
- [5] S.X. Dou, V. Braccini, S. Soltanian, R. Klie, Y. Zhou, S. Li, X.L. Wang, D. Larbalestier, J. Appl. Phys. 96 (2004) 7549.
- [6] K.P. Singh, V.P.S. Awana, Md. Shahabuddin, M. Husain, R.B. Saxena, Rashmi Nigam, M.A. Ansari, Anurag Gupta, Himanshu Narayan, S.K. Halder, H. Kishan, Mod. Phys. Lett. B 27 (2006) 1763.
- [7] Y. Zhu, L. Wu, V. Volkov, Q. Li, G. Gu, A.R. Moodenbaugh, M. Malac, M. Suenaga, J. Tranquada, Physica C 356 (2001) 239.
- [8] M. Delfany, X.L. Wang, S. Soltanian, J. Horvat, H.K. Liu, S.X. Dou, Ceram. Int. 30 (2004) 1581.
- [9] D.G. Hinks, J.D. Jorgensen, H. Zheng, S. Short, Physica C 382 (2002) 166.
- [10] I. Pallecchi, V. Braccini, E. Galleani d'Agliano, M. Monni, A.S. Siri, P. Manfrinetti, A. Palenzona, M. Putti, Phys. Rev. B 71 (2005) 104519.
- [11] Gaojie J. Xu, J.-C. Grivel, A.B. Abrahamsen, N.H. Andersen, Physica C 406 (2004) 95.
- [12] V.P.S. Awana, Rajeev Rawat, Anurag Gupta, M. Isobe, K.P. Singh, Arpita Vajpayee, H. Kishan, E. Takayama-Muromachi, A.V. Narlikar, Solid State Commun. 139 (2006) 306.
- [13] V.P.S. Awana, M. Isobe, K.P. Singh, Md. Shahabuddin, H. Kishan, E. Takayama-Muromachi, Supercond. Sci. Technol. 19 (2006) 551.
- [14] I. Felner, V.P.S. Awana, Monika Mudugul, H. Kishan, J. Appl. Phys. 101 (2007) 09G101.
- [15] C.P. Bean, Rev. Mod. Phys. 36 (1964) 31.
- [16] G. Blatter, M.V. Feigel'man, V.B. Geshkenbein, A.I. Larkin, V.M. Vinokur, Rev. Mod. Phys. 66 (1994) 1125.